Journal of
Ceramic Science
and Technology

J. Ceram. Sci. Tech., 07 [03] 235-242 (2016)
DOI: 10.4416/JCST2015-00073
available online at: http://www.ceramic-science.com

Synthesis and Characterization of Nanoparticulate Crystallite Cobalt Ferrite for Permanent Magnet Applications

M.A. Ahmed[1], N.G. Imam[*2], M.M. Hefny[3], and H.R. Gomaa[1]

[1]Materials Science Lab. (1) Physics Department, Faculty of Science, Cairo University, Giza, Egypt.
[2]Experimental Physics Department, Nuclear Research Center, Atomic Energy Authority, 13759, Cairo, Egypt.
[3]Chemistry Department, Faculty of Science, Cairo University, Giza, Egypt.

received November 4, 2015; received in revised form December 8, 2015; accepted February 10, 2016

Abstract

Nanoparticulate cobalt ferrite $CoFe_2O_4$ (COF) was successfully obtained at relatively low temperature by means of a facile chemical wet method, namely citrate auto-combustion. X-ray diffraction (XRD) analysis, transmission electron microscopy (TEM), Fourier Transform Infrared (FTIR), and Vibrating Sample Magnetometry (VSM) were carried out to study the structural and magnetic properties, respectively. The XRD results confirm the formation of single spinel phase of COF with an average lattice parameter (a) of 8.38 nm. XRD analysis revealed that the crystal size is about 43 nm, which is close to the particle sizes observed from TEM images (45.33 nm). The FTIR measurements between 400 and 4000 cm^{-1} confirmed the intrinsic cation vibrations of the spinel structure of COF. The experimental results have been explained on the basis of size and surface effects of the nanodimensional crystal of COF. The high coercivity of the prepared nanodimensional COF is the figure of merit for permanent magnets. Dielectric parameters and AC conductivity were measured as a function of temperature (300 – 800) K and frequency starting from 100 kHz up to 5 MHz. The conduction phenomenon was explained on the basis of the electron hopping model.

Keywords: Nanoparticulate, $CoFe_2O_4$, sol-gel precursor, structural, magnetic, dielectric.

I. Introduction

With their key characteristics, nanodimensional crystallite magnetic material systems have been recently used in a wide range of fields such as magnetic drug delivery, hyperthermia for cancer treatment, ferro fluids, magnetic storage data and many other applications [1]. Accordingly, nanodimensional magnetic particles can be considered a promising area for research because of their wide application in many important fields such as biomedical applications, industry and others [1]. On account of its combination of magnetic and electrical properties, ferrite has proven useful in many technological applications thanks to its remarkable properties such as significant saturation of magnetization, high electrical resistivity, low electrical losses, and good chemical stability [2]. On the basis of their crystal structure, ferrites are grouped into three classes namely hexagonal ferrite, garnet and spinel ferrite [3]. Spinel ferrites are widely studied on account of their numerous applications [4]. In this work, we prepared cobalt ferrite (COF) as a spinel ferrite or specifically inverse spinel ferrite. Generally, spinel ferrite has the formula MFe_2O_4 where both M and Fe represent divalent and trivalent cations respectively and M (as Co or Ni) cation occupies the tetrahedral site in the crystal structure while the Fe cation occupies the octahedral site [3]. A notable characteristic of this spinel structure is its ability to form an extremely wide variety of total solid solutions, which means that the composition of a given ferrite can be strongly modified while the basic crystalline structure remains the same [4]. This means that the general properties of the ferrite can be easily "tailored" with variation of its composition. One important way of modifying the properties is to use different synthesis methods and optimize the synthesis parameters [5]. In the crystal structure of spinel ferrite, the trivalent cations are generally smaller than the divalent ones, which leads to a certain tendency towards the inverse structure depending on the "elastic energy factor" (one of the main factors controlling cation distribution in the crystal structure of spinel ferrite) [6].

In this paper, we discuss one of these spinel ferrites ($CoFe_2O_4$) or COF with inverse spinel structure because of its moderate saturation magnetization, high electrical properties, high magneto-crystalline anisotropy, good mechanical properties and chemical stability. It is very important to pay attention to every property in the product to open up a new and wide field of potential applications.

II. Experimental Procedure

(1) Nano-$CoFe_2O_4$ (COF) preparation and characterization techniques

In this work, nano-COF was synthesized by means of the citrate-nitrates auto-combustion method (one of the

* Corresponding author: imam.eaea@gmail.com

known wet chemical methods) [7]. Using the wet chemical method has many advantages over other methods (e.g. the ceramic method) as it is considered clean, fast, simple, and cheap, while providing an opportunity to control the size of the prepared nanoparticles relatively (when no sintering or high temperature that can cause an increase in the particle size is required). All chemical materials used in preparation process were purchased from British Drug Houses (BDH). The starting materials used in the preparation were high-purity (99.9 % BDH) metal nitrates, i.e. cobalt nitrate and iron nitrate, and citric acid (as fuel) with high purity (for the formation of high-quality nanoparticles). Moreover, using distilled water for preparation of the solutions is important to reduce the chance of the presence of impurities in the final product. The solution was prepared with the molar ratio of citric acid to total moles of nitrates at 1:1 where the stoichiometric amounts of cobalt nitrate $Co(NO_3)_2{\cdot}6H_2O$ (5 g), ferric nitrate ($Fe(NO_3)_3{\cdot}9H_2O$) (13.88 g) and citric acid ($C_6H_8O_7{\cdot}H_2O$) (10.83 g) were used. The pH value of the prepared solution was adjusted to 7 with the drop-wise addition of ammonia (ammonium hydroxide 30 % (NH_4OH)) and stirring. The size and the properties of spinel ferrite nanoparticles depend to a large extent on the pH, fuel, and the metal nitrates to fuel ratio (the pH of the solution needs to be in the natural range to avoid formation of undesired amino complex or uncompleted precipitation of the metal ions). The neutral (pH = 7) solution of stoichiometric amounts of starting nitrates and citric acid was placed on a hot plate. First, any water present was evaporated, then, as a result of continuous heating, the gel was formed at approximately 90 °C. With continuous heating it began to dry until it became a viscous gel. The self-ignition reaction then took place at approximately 120 – 200 °C. Without further heating, the product formed is a "porous product" with tree-like grey fibres. The reaction was completed in 20 – 30 s, giving rise to a dark grey voluminous product (Fig. 1) with a structure similar to a branched tree (Fig. 1). Then the formed "tree" sample was ground to obtain fine grey powders of COF. The phases in the sample were identified with an X-ray diffractometer (XRD), model Bruker D8, with CuK_α radiation (λ = 1.5418 Å) in a wide range of Bragg's angle (2θ) from (20° – 80°) at room temperature. Instrumental broadening was taken into consideration in the computation of the FWHM of the X-ray peaks. A high-resolution transmission electron microscope (HR-TEM, Tecnai G20, FEI, Netherlands) was used for the purpose of imaging the shape, morphology and electron diffraction of the fine particles of the prepared COF. The molecular signature of the samples was confirmed by means of FTIR (Nicolet iS10 FT-IR spectrometer) studies. The magnetization, remnant field and the coercive field were measured by tracing M-H hysteresis loops for the powder samples at room temperature and a magnetic field up to 20 kOe, using the LDJ vibrating sample magnetometer (VSM) model 9600. The magnetic susceptibility was measured with the modified Faraday method at different temperatures ranging from 300 K – 700 K as a function of applied magnetic field intensity of 1340, 1660, and 1990 Oe. In this method there is a homogeneous field in the central region between two (flat) poles of an electromagnet. The RLC Bridge (Hioki model 3531, Japan) was used to measure the AC electrical resistivity as well as the dielectric constant ε' and dielectric loss factor ε'' of the investigated samples at different temperatures from room temperature up to 800 K at various frequencies from 100 kHz to 5 MHz. The electrical resistivity of the samples used was accurately measured on samples in the form of discs (pellets) measuring about 1 cm in diameter and 0.2 cm in thickness. The two surfaces of each sample were polished well, coated with silver paste and left to dry before the isolation between the two coated faces and the good conduction of each face were checked.

Fig. 1: Photo showing a branched voluminous COF product obtained from the gel at pH = 7.

III. Results and Discussion

(1) Structural characterization: X-ray diffraction (XRD)

Fig. 2 shows an XRD chart of the prepared samples, which confirms the existence of mono spinel phase of $CoFe_2O_4$ (COF) without any extra or secondary phases. All the peaks of the XRD pattern were indexed using Bragg's law. Phase identification was performed with JCPDS card number 22 – 1086. The broad peaks give an indication of the nanodimension of COF. The position of the peaks gives information about the planes present and its intensity indicate the most dominant peak (311) or in other words the 100 % peak (which was used to obtain the relative intensity of any other peaks present). In general, all the peaks present in the pattern assure the formation of cubic spinel ferrite structure. The average crystallite size of COF was determined using Scherrer's formula (as reported in [8]) to be 43 nm. The internal crystal lattice parameter "a" (a = 8.38) was also calculated from this equation [9]:

$$a = d_{hkl}{\cdot}(h^2 + k^2 + l^2)^{1/2} \quad (1)$$

where h, k, l are the Miller indices of the crystal planes and d_{hkl} is the interplanar distance for a given plane with Miller indices (hkl).

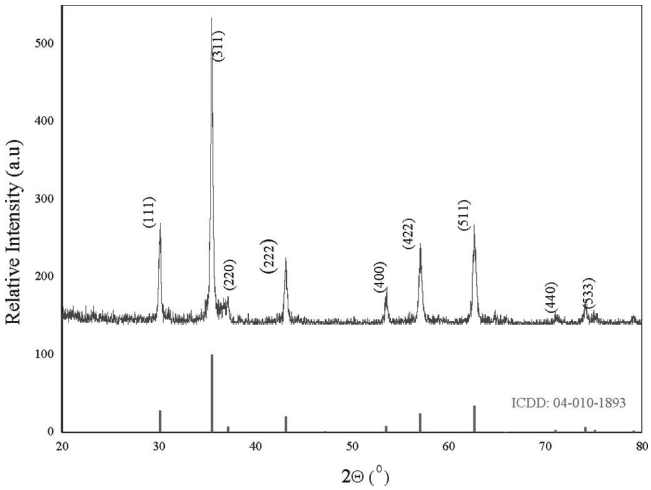

Fig. 2 : XRD pattern of Co-ferrite nanoparticles.

(2) High-resolution transmission electron microscopy imaging (HR-TEM)

Figs. 3a and b show HR-TEM two-dimensional images of the prepared COF with a clear view of the particles in the atomic scale and wide range of crystal size ranging from 13.94 nm to 72.1 nm. Analysis of the selected area diffraction (SAD) pattern confirms the presence of polycrystallite COF.

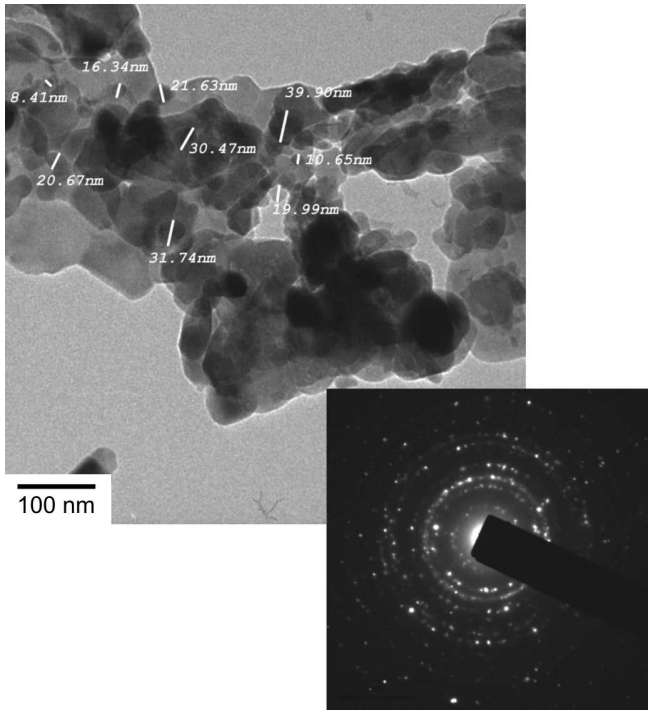

Fig. 3 : HR-TEM and SAED images of Co-ferrite nanoparticles.

(3) Fourier transform infrared (FTIR) spectroscopy

The FTIR spectroscopic technique is a very important tool to deduce the structural features and redistribution of cations between octahedral and tetrahedral sites [10] of the inverse spinel structures in COF nanoparticles. On studying the FTIR spectra of the COF, we may judge the iron ions contents on A- and B-sites. Then, magnetic properties can be evaluated non-quantitatively, because the distribution of metals ions on A- and B-sites determines the magnetic properties of spinel ferrite [8, 11]. The FTIR spectrum (Fig. 4) shows that the bands at 575.32, 591.64, 668.65 cm^{-1} are due to the stretching vibrations of the tetrahedral groups (Fe^{3+}-O^{2-}) [12]. The bands around 1384 cm^{-1}, 2341 cm^{-1} and 3735 cm^{-1} can be assigned to N-O stretching [12]. In addition, C-O bond [12], and O-H stretching bands respectively. These bands may be due to some powder from the sample in the wall of the beaker not being fired enough to remove N_2 and CO_2 completely [12].

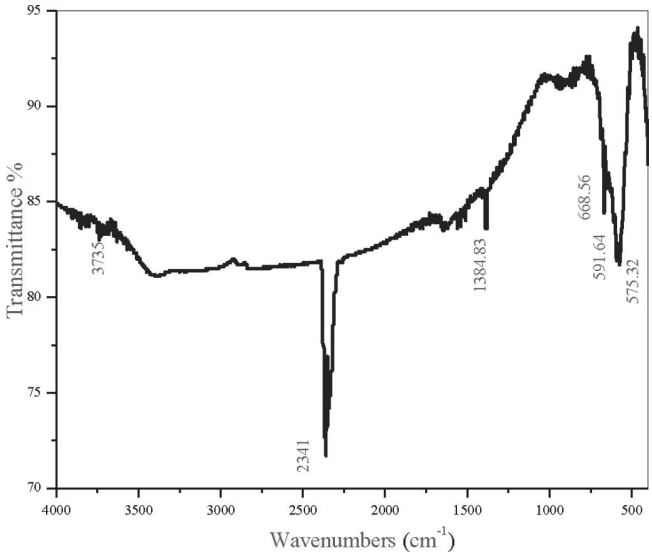

Fig. 4 : FT-IR spectrum of $CoFe_2O_4$ nanoparticles.

IV. Investigation of the Magnetic Properties of the COF Nanoparticles

The magnetic properties of the synthesized nano-dimensional COF were characterized by means of magnetic measurements; the molar magnetic susceptibility (χ_M) as a function of absolute temperature was measured at different magnetic field intensities. From the data of χ_M^{-1} vs. T, in the paramagnetic region, the effective magnetic moment and the Curie-Weiss constant could be easily calculated [13]. The hysteresis loop (M-H) at room temperature enables us to determine precisely the value of the saturation as well as the remnant magnetizations and coercive field [14].

Fig. 5a shows the relation between the molar magnetic susceptibility (χ_M) and absolute temperature ranging from 300 – 900 K as a function of the magnetic field intensity H (1010, 1340, and 1660 Oe.). The results show that the magnetic susceptibility (χ_M) of the ferrimagnetic COF increases with temperature up to the Curie temperature (T_C), however, COF loses its ferrimagnetic nature and become paramagnetic when the temperature exceeds T_C. This reduction in (χ_M) is attributed to the thermal agitation, which disturbs the oriented dipoles in random and different directions. Again, this reduction continues until T_C is reached at which the sample has completely changed from ferromagnetic to paramagnetic behaviour. This behaviour is typical of small magnetic particles and is considered to be due to blocking of individual particle magnetic moments along their anisotropy direction at

T = T_C [15]. The values for the Curie temperature were determined from the first derivative of magnetization (dM/dT) [16] as illustrated in Fig. 5b. The value of T_C that equals 825 °C represents the strength of characteristic A-B exchange magnetic interactions between the octahedrally and tetrahedrally coordinated cations, whereas the magnetic moments arrange themselves in an anti-parallel fashion [17]. It is observed that the T_C value is larger than that reported for bulk COF [17,18], which contributes to the effect of nanoscale on the magnetization of COF. Furthermore, the sudden reduction in molar magnetic susceptibility near T_C confirms the absence of impurities even in trace amounts, leading to the conclusion that a single spinel phase is formed as already predicted on the basis of the XRD analysis.

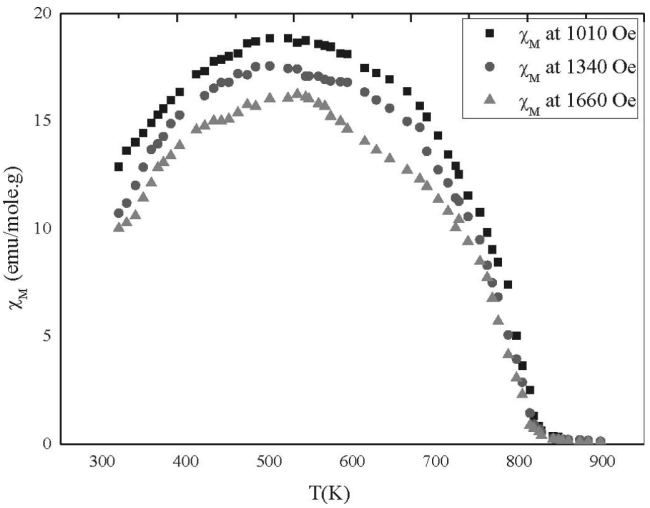

Fig. 5 a: The relation between the molar magnetic susceptibility and the temperature at different magnetic field intensity.

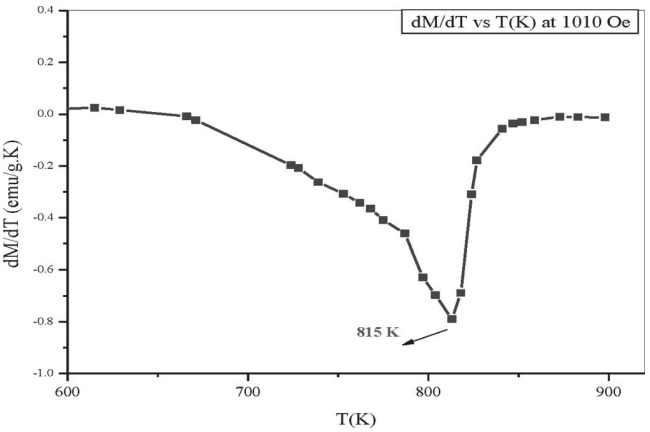

Fig. 5 b: Curie temperature T_C from the first order derivative of magnetization dM/dT.

The magnetic moment (n_B) in Bohr magnetron (the saturation magnetization per formula in Bohr magneton) at room temperature (300 K) is obtained from the magnetization data for all samples as calculated from the relation: $n_B = MM_s/5585$ [5], where M is the molecular weight and M_s is the saturation magnetization of the sample.

The reciprocal of the molar magnetic susceptibility was plotted versus absolute temperature in the paramagnetic region (Fig. 6). The data obeys the Curie-Weiss law; $\chi_M = C/T - (-\Theta)$[5], where χ_M is the magnetic molar susceptibility, C is the Curie constant, T is the absolute temperature and Θ is the Curie-Weiss constant. The values of Θ were calculated from the extrapolations of χ_M^{-1} in the paramagnetic region. The values of the effective magnetic moments are calculated from $\mu_{eff} = 2.83\sqrt{C}$ where C is the inverse of the slope of the straight line in the paramagnetic region, where it was found to be 7.75.

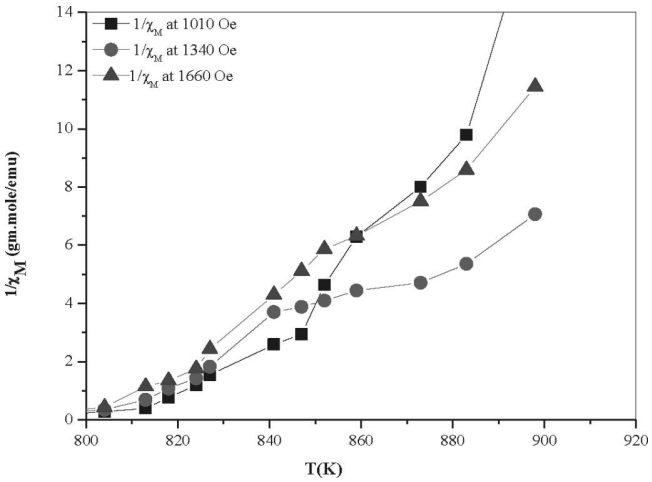

Fig. 6 : ($1/\chi_M$) vs. T(K) in the paramagnetic region.

(1) Vibrating scanning magnetometer (VSM)

Néel's model postulated that the ferrites are considered to possess a collinear ferrimagnetic structure in which the magnetization of the tetrahedral sub-lattice is anti-parallel to that of the octahedral (B) sub-lattice [18]. From magnetic hysteresis loop, the ferrimagnetic nature of synthesized COF is confirmed.

In Fig. 7, the typical room-temperature hysteresis loop of the nanodimensional COF shows the magnetization as a function of applied magnetic field to extract the magnetic parameters, including the saturation magnetization (M_s), coercive field (H_c), remanent magnetization (M_r), and squareness ratio (M_r/M_s). It is clear that the M-H loop confirms the ferromagnetic nature of nanodimensional COF. It is known that the magnetic parameter appears to be sensitive to cation distribution between the octahedral and tetrahedral sites. COF has an inverse-spinel structure, so that Co^{2+} ions are exclusively octahedrally coordinated, while Fe^{3+} ions are both tetrahedrally and octahedrally coordinated [1]. In the COF spinel, the Co^{2+} cations ($3d^7$, $4f^{9/2}$, L = 3, S = 3/2, and J = 9/2) have high spin ligand fields and possess 7d-electrons, three of which are unpaired. The obviously large magnetocrystalline anisotropy of COF nanoparticles evident in the large coercivity arises from the strong L-S couplings on the Co^{2+} cation sites [17,18]. A Fe^{3+} cation with $3d^5$ electron configuration tends to have its orbital angular momentum quenched in a weak ligand field [18]. Therefore, the contribution to the magnetic anisotropy should come from Co^{2+} cations. The M-H loop demonstrates the existence of stable ferrimagnetic fractions of COF ferrite materials at room temperature. The saturation magnetization (M_s), remnant magnetization (M_r)

and coercivity (H_c) of the investigated COF nanoparticles are 65.7 emu/g, 31.2 emu/g and 1373.1 G, respectively, while the value of the squareness ratio (M_r/M_s) is 0.475. The value of the squareness ratio reflects that the system consists of randomly oriented uni-axial particles with cubic magneto-crystalline anisotropy [19]. It is noted that the observed reduction of saturation magnetization value compared with the reported bulk value, i.e. ≈93 emu/g [5], is mainly owing to the thermal effects (superparamagnetism). The change in the magnetic structure on the surface of the nanodimensional material is significant owing to its large surface-to-volume ratio [19]. To account for the reduction in saturation magnetization in nanodimensional crystallite COF, canted spin structures on the surface layer of each crystallite composing a particle have been assumed [19]. Further, the reduction in saturation magnetization can also be attributed to the spin canting effect which arises from the lack of the balance exchange interaction for the magnetic ions on the surface of the nanoparticles [20]. The relatively high coercivity of the investigated COF is a fundamental characteristic property mainly because it is an important parameter for the maximum energy product (BH) max, the figure of merit for permanent magnets [17]. Furthermore, COF has large magnetocrystalline anisotropy [20] and reasonable magnetization, as potential predominant magnetic and electrical resistive materials that can be used in spintronic devices, high-density magnetic recording media, and high- performance electromagnetic as well as in catalytic applications [21]. The high coercivity essentially originates from the anisotropy of the cobalt ions at the octahedral (B) site owing to its important spin-orbit coupling [22].

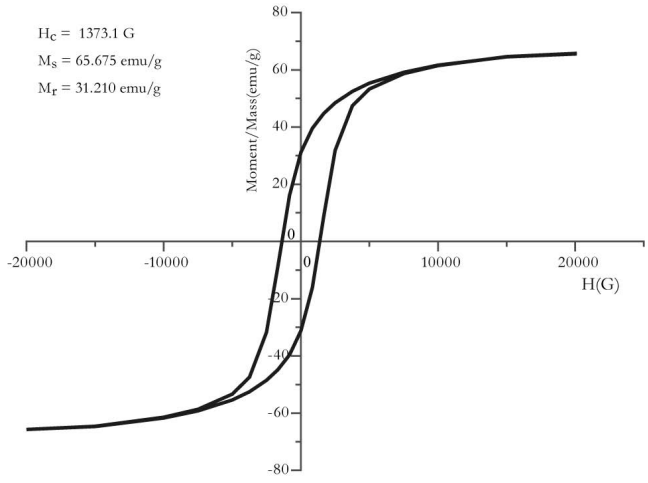

Fig. 7 : Room temperature hysteresis loop of Co-ferrite nanoparticles; the inset shows the magnetic parameters.

V. Dielectric Measurements of COF Nanoparticles

Ferrites are generally very good dielectric materials in low-frequency ranges, the dielectric behaviour of ferrites depending on factors such as method of preparation, chemical composition, chemical substitution, doping element, sintering temperature and grain structure or size [5]. Accordingly, COF has electrical properties that mainly depend on a number of parameters such as cation distribution, non-magnetic and magnetic substitution, amount of ferrous ions present, sintering conditions, grain size and grain growth effects [7]. From Fig. 8a, it can be observed that the dielectric constant decreases rapidly with an increase in the frequency and remains constant at higher frequencies, which is considered normal behaviour for a ferrite material and can be explained on the basis of the Maxwell theory [21] (the heterogeneous/interfacial polarization theory), which explains the ferrite materials as a solid material composed of well-conducting grains separated by insulating grain boundaries. At low frequency ranges, the conducting grains become active, promoting the hopping of electrons [22] (responsible for conduction in the ferrites). However, when the frequency increases beyond a certain value, the electron hopping cannot follow the frequency of the applied external field and polarization stagnates [22].

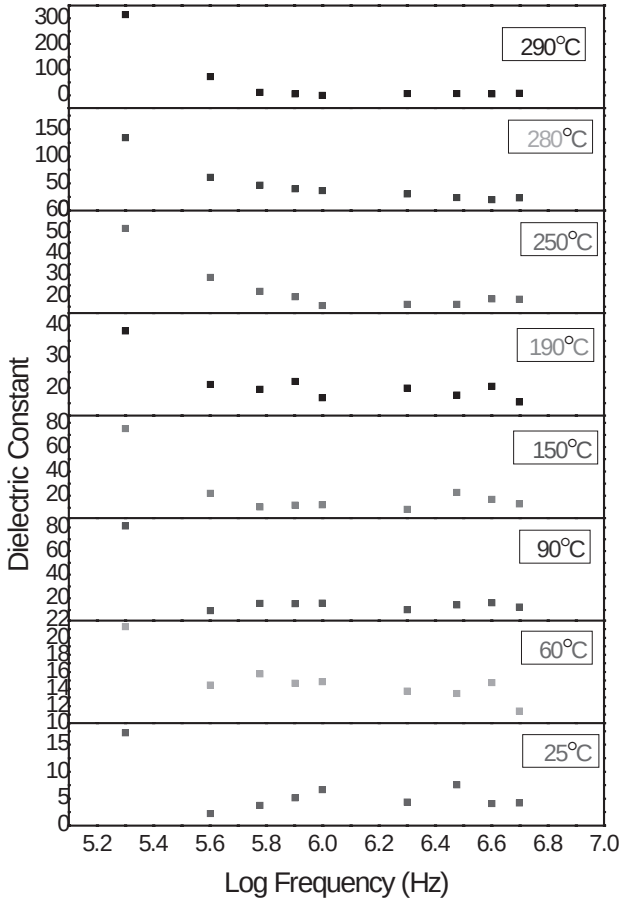

Fig. 8 a: Dielectric constant vs. Log Frequency at different temperatures.

Fig. 8b shows the relation between the dielectric constant and the absolute temperature (K). The dielectric constant remains low and constant for temperatures lower than 530 K, while increasing beyond this temperature to a maximum at 545 K at 0.8 MHz. This can be explained with the gradual rise in temperature, which thermally activates the hopping of charge carriers. Hence the dielectric polarization increases, thereby causing an increase in the dielectric constant [23].

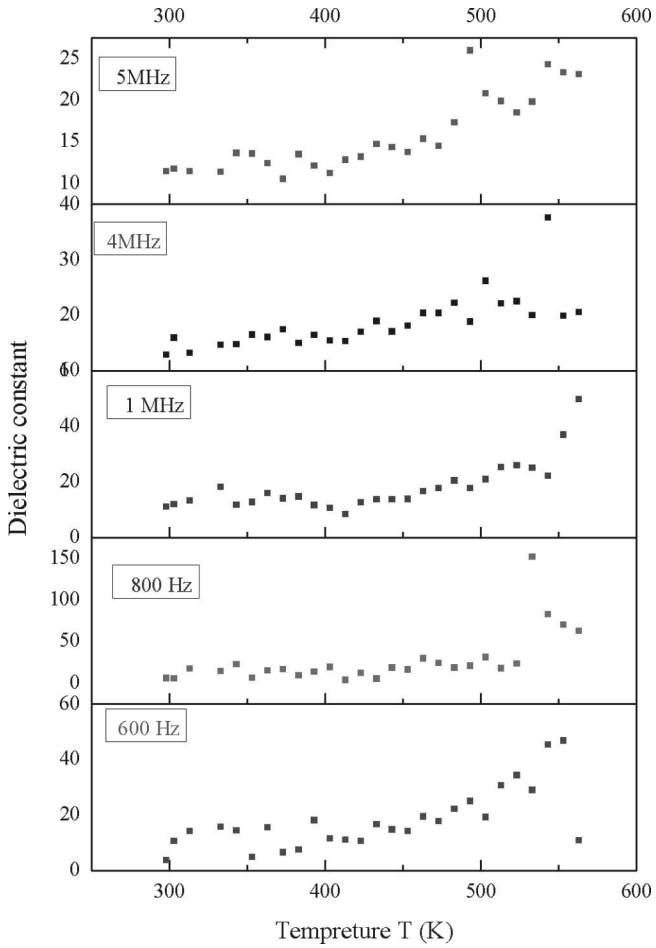

Fig. 8 b : Dielectric constant vs temperature at different frequencies.

A high value of ε′ is observed at lower frequencies, which falls rapidly with increasing frequency. This behaviour is typical of ferrites and a similar behaviour has been observed by several authors [22–24]. The trend can be explained on the basis that at lower frequencies, four different types of polarization contributions i.e. electronic, ionic, dipolar and space charge, play a part in the dielectric constant (ε′), but at higher frequencies some of the polarization contributions relax out, resulting in lowering of the dielectric constant (ε′) [24]. The decrease in dielectric constant (ε′) with increasing frequency is also explained on the basis of the fact that the frequency of electron hopping between the Fe^{2+} and Fe^{3+} ions at octahedral sites is higher than the applied *ac* field and can thus interact with the applied field easily, resulting in a higher value for the dielectric constant at lower frequencies. Contrary to this, at higher frequency the hopping electron cannot follow the frequency of the applied electric field, resulting in lowering of the dielectric constant. Consequently, the electron exchange between Fe^{2+} and Fe^{3+} is disturbed at high frequencies, which explains the slower decrease in the dielectric constant (ε′) at high frequency. Another possible explanation for the decrease in dielectric constant (ε′) with the frequency is given by Koops' model[25]. According to this model, the ferrite consists of two layers, the grains (a more conducting layer) and the grain boundaries (a poor conducting layer). In nanosized ferrites, the number of grain boundaries increases which contributes to the dielectric constant at lower frequencies while the grains have low dielectric constants and are effective at high frequencies. The variation in the dielectric constant as a function of the frequency reveals dispersion due to Maxwell-Wagner-type interfacial polarization, which is in good agreement with Koops' phenomenological theory [25]. According to this model, the COF ferrite structure is supposed to be composed of the fairly-well-conducting grains, separated by an ultra-thin insulating layer of grain boundaries. These grain boundaries could be formed either in each phase separately, owing to the superficial reduction or oxidation of crystallites in the porous materials as a result of their direct contact with the firing atmosphere during the sintering process.

VI. Conclusions

From the experimental results obtained, we can conclude the following:

Preparation of COF nanoparticulates with the citrate-nitrate auto-combustion method at relatively low temperature without further sintering was successful. The formation of single phase was confirmed with the XRD technique by determining the average crystal size of 43 nm. The chemical structure and the bonds formed were studied with FTIR, which confirmed the chemical structure of spinel ferrite of COF. High resolution for the formed semi-spherical cobalt ferrite was assured using HR-TEM imaging. The electrical and magnetic properties of COF were studied and the Curie temperature was determined at 513 K. Finally, the high values of coercivity and dielectric constant of the prepared nanodimensional COF is the figure of merit for permanent magnets. The novelty of this work is how to control the synthesis procedure to obtain nano-COF material at a certain size such that the high magnetic and dielectric parameters that characterize the bulk COF are still preserved in this nanomaterial with the advantage of a large surface-to-volume ratio to enhance its efficiency in different applications, since COF is still very important material particularly on nanoscale for modern technological and medical applications.

Acknowledgment

The authors would like to send a message to Prof. DSc. Mohamed Ali Ahmed to tell him that he is still alive with us and we cannot forget him, he is in our hearts forever. Thank you M.A. Ahmed.

References

1 Sangmanee, M., Maensiri, S.: Nanostructures and magnetic properties of cobalt ferrite (CoFe2O4) fabricated by electrospinning, *Applied Phys. A – Mater.*, **97**, 167 – 177, (2000).

2 El-Shobaky, G.A., Turky, A.M., Mostafa, N.Y., Mohamed, S.K.: Effect of preparation conditions on physicochemical, surface and catalytic properties of cobalt ferrite prepared by co-precipitation. *J. Alloy Compd*., **493**, 415 – 422, (2010).

3 Imam, N.G., Ismail, S.M., Yehia, M., Hashhash, A.: Photoluminescence, magnetic and electrical properties of Co-ferrite nanoparticles synthesised via sol-gel auto-combustion method, *Int. J. Nanoparticles*, **7**, [3 – 4], (2014), doi: 10.1504/IJNP.2014.067601.

4 Amiri, S., Shokrollah, H.: Magnetic and structural properties of RE doped Co-ferrite (RE = Nd, Eu, and Gd) nanoparticles

synthesized by co-precipitation, *J. Magn. Magn. Mater.*, **345**, 18 – 23, (2013).

5 Ahmed, M.A., Okasha, N., Imam, N.G.: Advanced imaging techniques for characterization of $0.5BaTiO_3/0.5Ni_{0.5}Zn_{0.5}Fe_2O_4$ multiferroic nanocomposite, *J. Alloy. Compd*., **557**, 130, (2013).

6 Singh, R.K., Narayan, A,. Prasad, K.: Thermal, structural, magnetic and photoluminescence studies on cobalt ferrite nanoparticles obtained by citrate precursor method, *J. Therm. Anal. Calorim.*, **110**, (2012), 573 – 580, doi: 10.1007/s10973 – 012 – 2728 – 1.

7 Ahmed, M.A., Okasha, N., Imam, N.G.: Crossover between PEG and BT/NZF Magnetoelectric nanocomposite for tailoring applicable multiferroic materials, *J. Supercond. Nov. Magn.*, **28**, [9], 2783 – 2793, (2015), DOI: 10.1007/s10948 – 015 – 3115 – 5.

8 Ahmed M.A., Imam, N.G., El-Dek, S.I., Safaa K. El-Mahy: Fluorescence and spectroscopic characterization of multiferroic quantum dots of La:$BiFeO_3$, *J. Supercond. Nov. Magn.*, (2015), doi: 10.1007/s10948 – 015 – 3027 – 4.

9 Ahmed, M.A., Imam, N.G., Abdelmaksoud, M.K. SaeidY.A.: Magnetic transitions and butterfly-shaped hysteresis of Sm-Fe-Al-based perovskite-type orthoferrite, *J. Rare Earth*, **33**, [9], 965, (2015).

10 Heiba, Z.K., Imam, N.G., Mohamed, M.B.: Temperature dependent cation distribution correlated with optical and magnetic properties of nanocrystalline $NiFe_{1.8}Gd_{0.2}O_4$, *J. Mol. Struct.*, **1095**, 61 – 68, (2015). http://dx.doi.org/10.1016/j.molstruc.2015.04.020.

11 Ahmed, M.A., Seddik, U., Okasha, N., Imam, N.G.: One-dimensional nanoferroic rods; synthesis and characterization, *J. Mol. Struct.*, **1099**, 330 – 339, (2015), doi:10.1016/j.molstruc.2015.05.060.

12 Zhao, L., Zhang, H., Xing, Y., Song, S., Yu, S., Shi, W., Guo, X., Yang, J., Lei, Y., Cao, F.: Studies on the magnetism of cobalt ferrite nanocrystals synthesized by hydrothermal method, *J. Solid State Chem.*, **181**, 245 – 252, (2008).

13 Ahmed, M.A., Okasha, N., Imam, N.G.: Structural and magnetic properties of electroceramic magnetoelectric nanocomposites, The African Review of Physics, ICTP, Italy, **7**, [2], 7 – 17, (2012) doi:http://www.aphysrev.org/index.php/aphysrev/article/view/516/222.

14 Imam, N.G., Bakr Mohamed, M.: Optical properties of diluted magnetic semiconductor Cu: ZnS quantum dots, *Superlattice. Microst.*, **73**, 203 – 213, (2014) 205. doi: http://dx.doi.org/10.1016/j.spmi.2014.05.026.

15 Chen, J., Wang, Y., Deng, Y.: Highly ordered $CoFe_2O_4$ nanowires array prepared via a modified sol-gel templated approach and its optical and magnetic properties. *J. Alloy Compd*., **552**,65 – 69, (2013).

16 Ahmed, M.A., Okasha, N., Imam, N.G.: Modification of Composite Ceramics Properties via Different Preparation Techniques, *J. Magn. Magn. Mater. (MAGMA)*, **324**, 4136 – 4142, (2012).

17 Manikandan, A., John Kennedy, L., Bououdina, M., Vijaya, J.J.: Synthesis, optical and magnetic properties of pure and Co-doped ZnFe2O4 nanoparticles by microwave combustion method, *J. Magn.Magn. Mater.*, **349**, 249 – 258, (2014).

18 Kundu, A., Upadhyay, C., Verma. H.C.: Magnetic properties of a partially inverted zinc ferrite synthesized by a new co-precipitation technique using urea, *Phys. Lett. A*, **311**, [4 – 5], 410 – 415.

19 Wahba, A.M., Imam, N.G., Mohamed, M.B.: Flower-like morphology of blue and greenish-gray $ZnCo_xAl_{2-x}O_4$ nanopigments, *J. Mol. Struct.*, **1105**, 61 – 69, (2016), doi: 10.1016/j.molstruc.2015.10.052.

20 Peddis, D., Yaacoub, N., Ferretti, M., Martinelli, A., Piccaluga, G., Musinu, A., Cannas, C., Navarra, G., Greneche, J.M., Fiorani, D.: Cationic distribution and spin canting in $CoFe_2O_4$ nanoparticles, *J. Phys. - Condens. Mat.*, **23**, 426004 (8pp), (2011).

21 Aljuraide, N.I., Mousa, M.A.A., Mostafa, N.Y., El-Shobaky, G.A., Hamdeh, H.H., Ahmed, M.A.: Microstructure analysis of zinc ferrite nanoparticles by means of X-ray powder diffraction and Mössbauer spectroscopy, *Int. J. Nanoparticles*, **5**, 56 – 63, (2012).

22 Ahmed, M.A., Seddik, U., Imam, N.G.: First-order studies of nanometric biferroic, WJCMP, 2, [2], 66 – 74, (2012). *doi: 10.4236/wjcmp.2012.22012*.

23 Amiri, S., Shokrollahi, H.: Magnetic and structural properties of RE doped Co-ferrite (RE = Nd, Eu, and Gd) nanoparticles synthesized by co-precipitation J. *Magn. Magn. Mater.*, **345**, 18 – 23, (2013).

24 Ahmed, M.A., Okasha, N., Imam N.G.: Novel behavior of the transport properties of magnetoelectric (ME) nanocomposite, *PJETR*, **1**, 19 – 25, (2012).

25 Koops, C.G.: On the dispersion of resistivity and dielectric constant of some semiconductors at audio frequencies, *Phys. Rev.*, **83**, [1], 121 – 124, (1951), doi:10.1103/PhysRev.83.121.